

Distribution changes of woody plants in Western Iran as monitored by remote sensing and geographical information system: a case study of Zagros forest

Mansour Karkon Varnosfaderani¹ · Rasoul Kharazmi² · Aliakbar Nazari Samani³ · Mohammad Reza Rahdari³ · Seid Hamid Matinkhah⁴ · Nasrollah Aslinezhad⁵

Received: 16 February 2015 / Accepted: 12 December 2015 / Published online: 27 June 2016
© Northeast Forestry University and Springer-Verlag Berlin Heidelberg 2016

Abstract The status of woody plants in dry-land systems is a fundamental determinant of key ecosystem processes. Monitoring of this status plays an important role in understanding the dynamics of woody plants in arid and semi-arid ecosystems. The present study determined the dynamism of the Zagros forests in Iran using Remote Sensing and Geographic Information System techniques and statistical science. The results show that the density of trees varied from 10 to 53 % according to the physiographic and climatic conditions of semi-arid regions. The best and lowest correlation between vegetation indices and forest density were obtained for the global environmental monitoring index (GEMI; $R^2 = 0.94$) and soil adjust vegetation index ($R^2 = 0.81$), respectively. GEMI is used to monitor land use changes over a 10-year period. Results show that 2720 ha² of forest have been destroyed by human interference and tillage on steep slopes during this period which also resulted in the loss of the fertile soil layer. GEMI determined the areas with a biomass of trees

and could normally separate border regions with low biomass density of trees from regions without canopy cover. The results revealed that assessment of forest and vegetation cover in arid and semi-arid arduous forest regions using satellite digital numbers and ordinary sampling is subject to uncertainty. A stratified grouping procedure should be established to increase the accuracy of assessment.

Keywords Monitoring · Woody plants · Vegetation index · RS · GIS · Zagros forest · Iran

Introduction

Arid and semi-arid ecosystems are those in which the ratio of total annual precipitation to potential evapotranspiration is 0.05–0.50; these areas cover about 30 % (about 4 billion ha²) of global dry land (Beadle 1959; Bailey 1979; Paruelo et al. 2000; Diouf and Lambin 2001; Lal 2004; Austin and Vivanco 2006; Heisler-White et al. 2008; Rotenberg and Yakir 2010; Walker 2012; Riha et al. 2014; Letnic et al. 2015). Vegetation in dry-land ecosystems support global biodiversity, carbon sequestration, and the majority of the world's livestock. The woody plant mosaic in dry-land ecosystems is a fundamental determinant of key ecosystem processes (e.g., evapotranspiration, fire disturbance) and associated abiotic patterns (Breshears 2006).

Monitoring long-term changes in an ecosystem over large spatial extents is critical for understanding the dynamics of woody plants in arid and semi-arid ecosystems and their responses to natural disturbance and rangeland management (Jian et al. 2012; Saranya et al. 2014). Monitoring long-term tree cover dynamics in semi-arid woodlands requires repeated retrieval of the tree canopy cover

The online version is available at <http://www.springerlink.com>

Corresponding editor: Yu Lei

✉ Mohammad Reza Rahdari
rahdari@ut.ac.ir; rahdarimr@gmail.com

¹ State University of Land Use Planning, Moscow, Russian Federation

² St.Petersburg State University, Petersburg, Russian Federation

³ Faculty of Natural Resource, University of Tehran, Karaj, Iran

⁴ Isfahan University of Technology, Isfahan, Iran

⁵ Faculty of Water and Soil, Zabol University, Zabol, Iran

area with relatively high accuracy (Hostert et al. 2003; Cohen et al. 2003; Jian et al. 2012).

Field measurement of the tree canopy cover is expensive, labor-intensive, and often limited in temporal scope and spatial scale. Remote sensing (RS) has been demonstrated to be a suitable alternative for quantifying biophysical variables such as leaf area index and vegetation cover (Cohen et al. 2003; Tang et al. 2014; Béland et al. 2014). Tree canopy cover in dry land ecosystems can be confounded by shrub cover and can contribute considerably to leaf area and foliar biomass. Quantifying tree canopy cover in dry land ecosystems using RS data can be particularly challenging in areas with low tree cover and density, short tree stature, and coexistence of trees and shrubs at fine spatial scales (Ko et al. 2009). In arid and semi-arid regions, changes in woody plant cover have dramatic effects on ecosystems (Breshears 2006; Homet-Gutiérrez 2015). RS has been used to provide spatially explicit information about the heterogeneity of woody plant distribution over extensive dry land areas (Walker et al. 2012; Ferreira et al. 2015).

Landsat archival imagery (LAI) can be effective for monitoring woodland expansion and contraction in semi-arid landscapes over time (Zhu et al. 2012; Jian et al. 2012; Griffiths et al. 2014; Schmidt et al. 2015). Studies on different biomes, including cropland, plantations, and forests (conifer and deciduous stands) have successfully linked LAI measurements on the ground using direct or indirect techniques to RS data (Chen and Black 1991; Chen and Cihlar 1996; Colombo et al. 2003; Brantley et al. 2011). About 300 vegetation indices have been published; however, only a few of those based on biophysics or on specific methods have been adopted (Thenkabail et al. 2016). These studies correlate spectral vegetation indices (SVIs) from different types of satellite data (Adina et al. 2014). The most popular of these indices are the normalized difference vegetation index (NDVI), simple ratio (SR) index, and soil-adjusted vegetation index (SAVI).

The relationship between LAI and different combinations of SVIs has been analyzed in a variety of studies (Adina et al. 2014; Le Maire et al. 2011). Besides linear, quadratic polynomial, and cubic polynomial links, most studies have shown logarithmic relationships (Tucker 1979; Myneni et al. 1997; Chen and Cihlar 1996; Datt 1999; Mutanga and Skidmore 2004; Le Maire et al. 2011; Potitthep et al. 2013). Time series analyses provide powerful alternatives with their ability to separate seasonal variation from long-term trends (Sulla-Menashe et al. 2014; Lanorte et al. 2014; Starr et al. 2015; Ahmed et al. 2015). Trend analysis has been frequently applied to characterize land surface phenology change from coarse-scale imagery (Slayback et al. 2003; Heumann et al. 2007; Bradley and Mustard 2008).

Our study tested instrumental and technological solutions that efficiently and accurately describe desertification dynamics through creation of vegetation degradation maps for rational management. Multispectral Landsat images and calculation of vegetation indices were chosen to accommodate the large area of the study site in the Zagros forest of Lorestan to decrease the cost of processing the technology. Field studies were carried out at single research sites using optimal vegetation index to extract results for desertification of the region. In past decades, deterioration of vegetation and land degradation in arid and semi-arid regions has forced the managers to use new and rapid technology to extract vegetation maps on local and regional levels for monitoring and assessment. This ability increases understanding of the influences of humans and climate change on land degradation. It is crucial to calibrate and determine the best indices to obtain reliable results about the status of the vegetation.

Materials and methods

Study area

The study area is located in western Iran at 48°47'–50°3' longitude and 32°44'–33°35' latitude. This includes part of the central Zagros forests with an area of 32,231 ha (Fig. 1). Geomorphologic classification of area is mountainous and its climate is semi-humid cold. The species in order of frequency are *Quercus brantii*, *Daphne mucronata*, *Amygdalus scoparia*, *Acer monspessulanum*, *Amygdalus lycioides*, *Cerasus brachypetala*, *Crataegus pontica*, *Amygdalus orientalis*, *Pistacia mutica*, and *Pistacia khinjuk* (Henareh Khalyani et al. 2012; Ghanbari and Sefidi 2012).

Methodology

Our study improved the compatibility of the vegetation index (Table 1) with trends in the environment, climate, and cover change over a 10-year period from 2002 to 2013. Satellite imagery for the years 2002 (Landsat 5, TM), 2009 (Landsat 7, ETM⁺), and 2013 (Landsat 7 ETM⁺) with a spatial resolution of 30 m² were used (Huang et al. 2009; Brandt et al. 2012). All images were recorded in the month of July to increase accuracy by comparison of similar time frames. Two topographic map sheets were used to identify and visit the area and as ground truth maps. Topographic map sheets were applied to identify ground control points to allow geometric correction of the satellite images and evaluate the accuracy of the geometric correction.

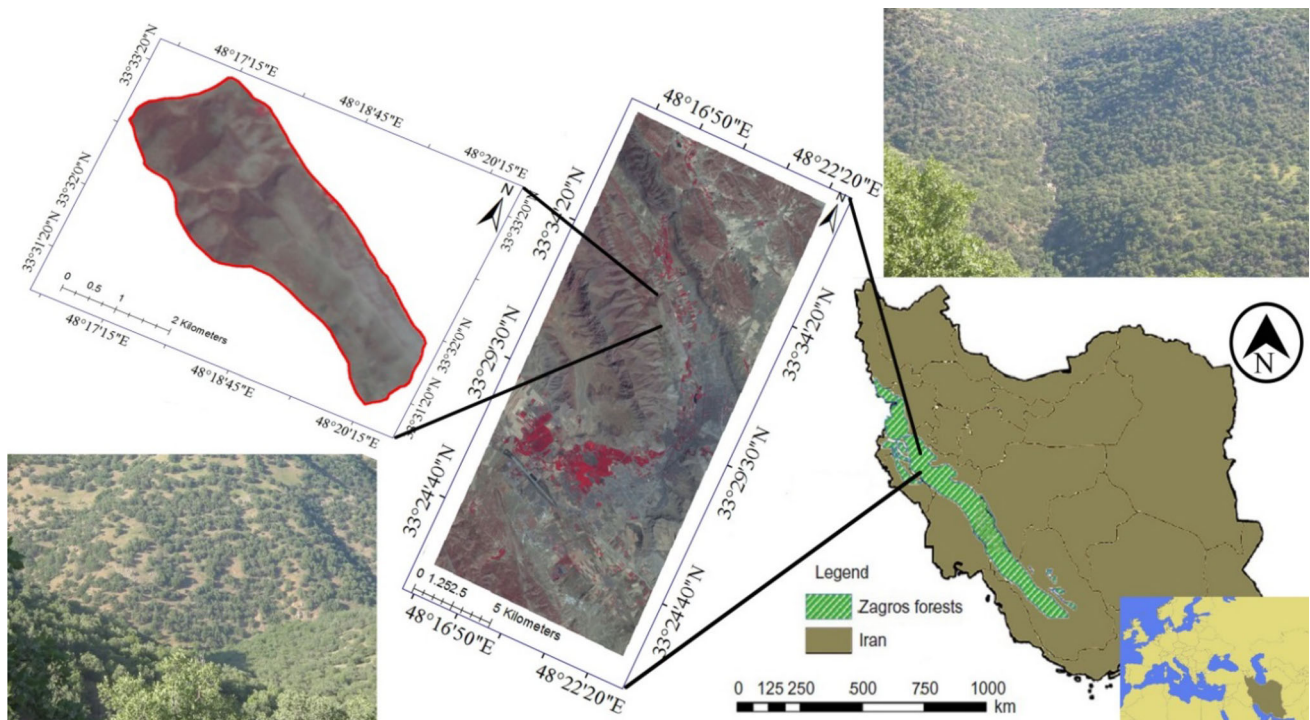


Fig. 1 Location of Zagros forests and study area in Iran

Table 1 Spectral vegetation indices

Equations	Vegetation index (VI)	Authors
$NDVI = \frac{NIR-RED}{NIR+RED}$	Normalized VI	Rouse (1974)
$IPVI = \frac{NIR}{NIR+RED}$	Infrared percentage VI	Crippen (1990)
$SAVI = \frac{NIR-RED}{NIR+RED+L} \times (1+L)$	Soil adjusted VI	Huete (1988)
$MSAVI2 = \frac{NIR-RED}{NIR+RED+L} \times (1+L)$	Modified soil adjusted VI	Qi et al. (1994)
$L = 1 - \frac{2 \times NIR + 1 - \sqrt{(2 \times NIR + 1)^2 - 8 \times (NIR \times RED)}}{2}$		
$GEMI = E \times (1 - 0.25 \times E) - \frac{(RED - 0.125)}{1 - RED}$	Global environmental monitoring index	Pinty and Verstraete (1992)
$E = \frac{2 \times (NIR^2 - RED^2) + 15 \times NIR + 0.5 \times RED}{NIR + RED + 0.5} \times (1 + L)$		
$EVI = \left\{ \frac{NIR-RED}{NIR+C1 \times RED - C2 \times BLUE+L} \right\} \times (1+L)$	Enhanced VI	Rouse (1974)

Randomized systematic sampling was used in this study. The distance between the UTM grid lines was 1 km. The line transect method was used with a starting point for each transect at the cross point at the 1 km × 1 km grid lines for the 1:25,000 scale maps with forest coverage. Along each transect, every single tree or shrub species having crowns that intersect the line transect were listed by scientific name. The understory species at each transect were recorded as an index of human influence. The length of each transect depended on the density of the forest canopy. For canopy cover of <10, between 10 and 50, and >50 %, the cover transect length was 100, 200, and 400 m, respectively. The data was managed in the form of a

database that was built, sorted, and filtered using Microsoft Access software. Descriptive statistical parameters such as the total number of each species, means, extremes, frequency histograms were helpful for analysis of the niches of the plants.

Because the images sent from the satellite were received at different moments, it is necessary to compare the vegetation indices by converting the digital number (DN) of the satellite images to spectral reflectance (Coppin et al. 2004; Macleod and Congalton 1998; Singh 1989). Atmosphere conditions (humidity, height of sun, azimuth of sun, accurate timing of images) from the Scanex image processing software were used to account for the effect of

atmosphere on surface reflectance. It is crucial to remove the effects of atmosphere, but is not possible to assess it precisely without time data on atmospheric conditions in countries such as Iran. The following algorithm was used to convert the DN to spectral reflectance (Richards 1993; Lillesand and Kiefer 1994; Roni 2013):

$$L = L_{\min} + (L_{\max} - L_{\min})/1023 \times DN \quad (1)$$

where L is spectral radiance, L_{\min} is 1.238 (spectral radiance of DN 1), L_{\max} is 15.600 (spectral radiance of DN 255) and:

$$\rho_p = \frac{\pi \times L_\lambda \times d^2}{ESUN_\lambda \times \cos \theta_s} \quad (2)$$

where ρ_p is the unitless planetary reflectance, L_λ is the spectral radiance at the sensor aperture, d is the distance from the earth to the sun in astronomical units from a nautical handbook, $ESUN_\lambda$ is the ALI solar irradiance, and θ_s is the solar zenith angle in degrees. The following formula was proposed for field research for the average percentage of vegetation cover in transects (Franklin 2001):

$$F = \frac{78.5T \sum CD}{L} = \sum CD \quad (3)$$

where CD is the perpendicular diameter of the canopy cover of trees at the test points, $T \sum CD$ is total CD located on the transects, L is the length of the transect, and F is the density of the tree canopy on the transects. Relation 3 was

Table 2 Total biomass density of trees (%) at all test points on 7 transects

Transect	L	$T \sum CD$	Density of trees (%)
1	100	67.9	53.3015
2	200	88	34.54
3	200	107.2	42.076
4	100	51.6	40.506
5	400	89.6	17.584
6	200	28.02	10.99785
7	200	97.05	38.09213

Table 3 Average numerical value of each vegetation index at all test points on 7 transects

Transects	EVI	GEMI	IPVI	MSAVI2	NDVI	SAVI ($L = 0.5$)	SAVI ($L = 1$)
1	0.192	0.459	0.605	0.144	0.211	0.158	0.14
2	0.121	0.403	0.571	0.087	0.143	0.099	0.086
3	0.147	0.421	0.583	0.106	0.166	0.118	0.103
4	0.165	0.438	0.598	0.116	0.197	0.132	0.113
5	0.1	0.351	0.554	0.08	0.108	0.087	0.079
6	0.099	0.342	0.551	0.076	0.101	0.082	0.075
7	0.167	0.438	0.594	0.12	0.188	0.134	0.117

used to calculate the biomass density of the trees at the test points on the transects.

Geographical coordinates were recorded by GPS in the statistical test and arc GIS 10.2 software was used to convert the geographical coordinates of the test points to vector points using Scanex. The components of each vector point in the vegetation indices were extracted separately. The average values of each vegetation indices of test points and RMSE for the transects were calculated to select the appropriate vegetation index regression formula, error coefficient, correlation coefficients of the total biomass density of the trees of all test points located in the experimental transects.

Results

The total biomass density of the trees (percentage) at all test points for the 7 transects are shown in Table 2 and the average numerical values of each vegetation index are shown in Table 3.

Correlation diagrams for each indicator versus the biomass density of the trees are shown in Fig. 2. These regression diagrams were obtained using the data from more than 135 test points along the seven transects to calculate the numerical values of each vegetation index using the average values at select test points on each transect. The result shows the highest correlation coefficient, description coefficient, and the lowest RMSE for GEMI versus the density of the forest cover obtained from field calculation (Table 4).

A small boundary was chosen as the control area. Aerial photographs, Google Earth software, and the results of the field study were visually interpreted and the forest area was separated from bare land and imported into the software. The area of the control step was 577.3 ha² (Table 5).

A map of the control area was created for the indices using Scanex to determine the relation between the accuracy of the forest area and the indices (Fig. 3). A visual comparison of the maps (forest vegetation indices) results in percentages of <30 % for bare land, 30–75 % for forest, and 75–100 % for irrigated area. The result shows that

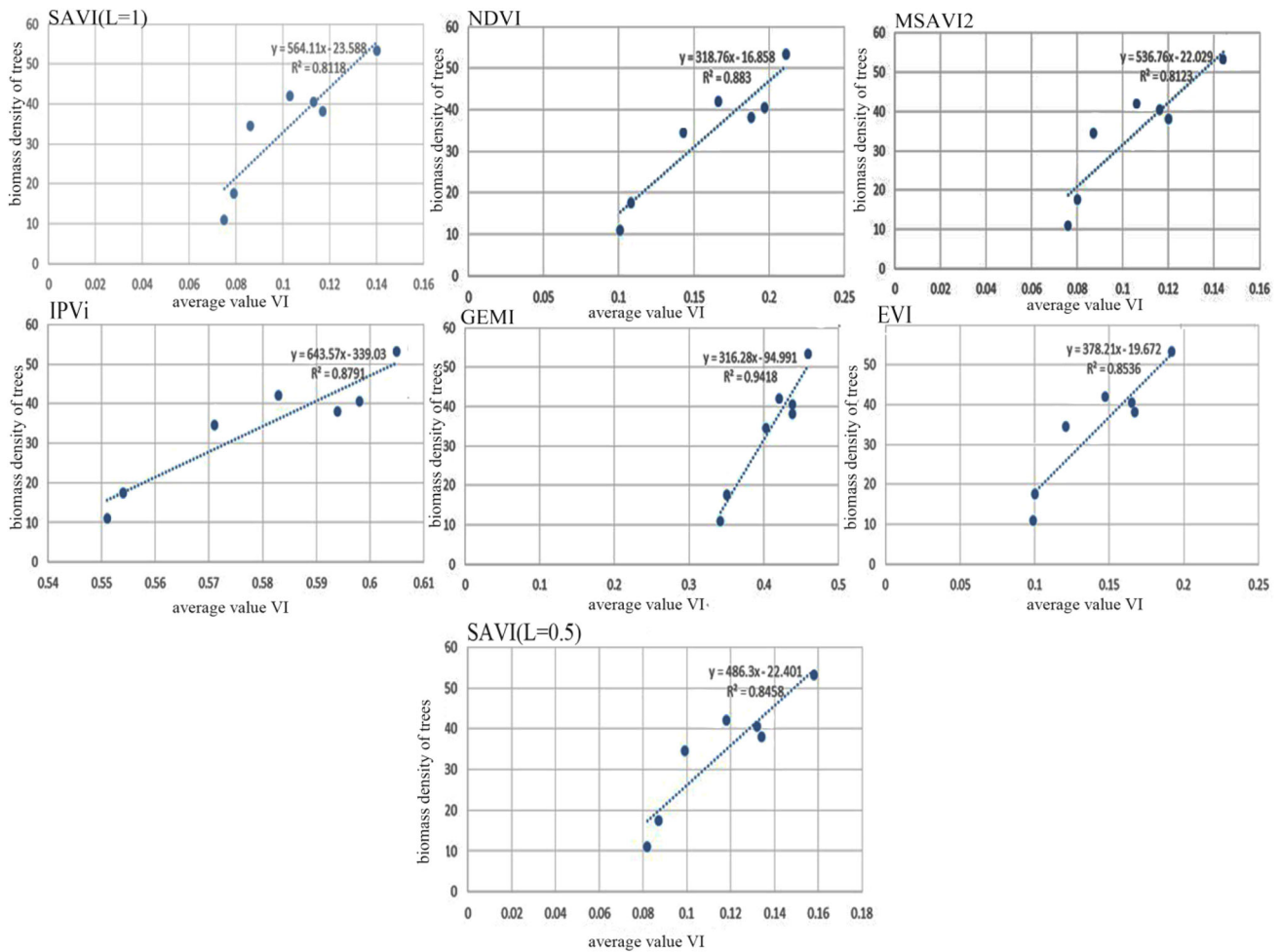


Fig. 2 Correlation diagrams for each indicator versus biomass density of trees

Table 4 Results of linear regression analysis and RMSE

Vegetation indices	Vegetation model	Description coefficient (R^2)	RMSE	Correlation coefficient
EVI	$Y = 378.21X - 19.672$	0.85	0.28	0.92
GEMI	$Y = 316.28X - 94.991$	0.94	0.02	0.97
IPVi	$Y = 643.57X - 339.03$	0.88	0.04	0.94
MSAVI2	$Y = 536.76X - 22.029$	0.81	0.05	0.9
NDVI	$Y = 318.76X - 16.858$	0.88	0.04	0.94
SAVI ($L = 0.5$)	$Y = 546.11X - 23.558$	0.84	0.043	0.92
SAVI ($L = 1$)	$Y = 486.3X - 22.401$	0.81	0.04	0.9

The numerical value (Y) for the vegetation indices with canopies of 1, 5, 10, 30, 50, 75 and 100 % in Table 5

GEMI was more accurate than the other indices used to calculate the forest area of each indicator by visual interpretation (Table 6).

GEMI provided the most appropriate correlation for forest area to detect changes in forest area over a 10-period (Table 7). Satellite images for 2002 and 2013 from ETM⁺ (Landsat 7) were used to extract the vegetation indices for each image (Fig. 4).

Discussion and conclusion

The results show that GEMI was the best choice for detecting changes in the study area and other areas (Torahi and Rai 2011; Jian et al. 2012; Henareh Khalyani et al. 2012; Adina et al. 2014). GEMI ($R^2 = 0.94$) was chosen because it produced the greatest accuracy and ability to separate the border of the canopy cover of trees. It was

Table 5 Vegetation indices for different canopies

Indices	1 %	5 %	10 %	30 %	50 %	75 %	100 %
NDVI	0.056	0.068	0.084	0.147	0.21	0.288	0.367
GEMI	0.303	0.316	0.332	0.395	0.459	0.537	0.616
IPVI	0.528	0.534	0.542	0.573	0.604	0.643	0.682
SAVI_0.5	0.049	0.056	0.066	0.108	0.149	0.2	0.252
MSAVI2	0.043	0.05	0.06	0.097	0.134	0.181	0.227
SAVI_1	0.043	0.05	0.059	0.095	0.13	0.174	0.219
EVI	0.055	0.065	0.078	0.131	0.184	0.25	0.316

used to create a formula for calculating the biomass density of trees based on the geo-ecology of the study region. GEMI has been empirically shown to be insensitive to atmospheric influences, but other drawbacks to the index have not been uncovered. The value from GEMI correlated highly with the field survey and was able to determine the area of the biomass of trees. It can normally divide border

regions with the low biomass density of trees from regions without canopy cover.

SAVI ($R^2 = 0.81$) for $L = 1$ showed the lowest correlation related to its maximum value of coefficient L as applied to arid land; this was a result of the minimizing effects of soil spectral reflectance (Colombo et al. 2003). NDVI was acceptable in most studies with relatively good coverage (Peters et al. 2002) and EVI was good for forest area (Chaban 2004; Galvao et al. 2011), but had a lower correlation in the study area ($R^2 = 0.88$) than GEMI. This could be the result of the higher impact factor in the near-infrared band in GEMI (the band in which vegetation has high reflectance).

Semi-arid woodland areas (such as the oak forest of western Iran) showed a diversity of ground cover along the transects together with GPS accuracy. It can produce high uncertainty when relying on the statistical analysis of a single pixel data. The averages of the records in each transect were used to cover spatial variation and the results revealed better correlation in some area, such as Zagros forest, in arid and semi-arid areas.

Fig. 3 Cover classes based on indices versus visual interpretation

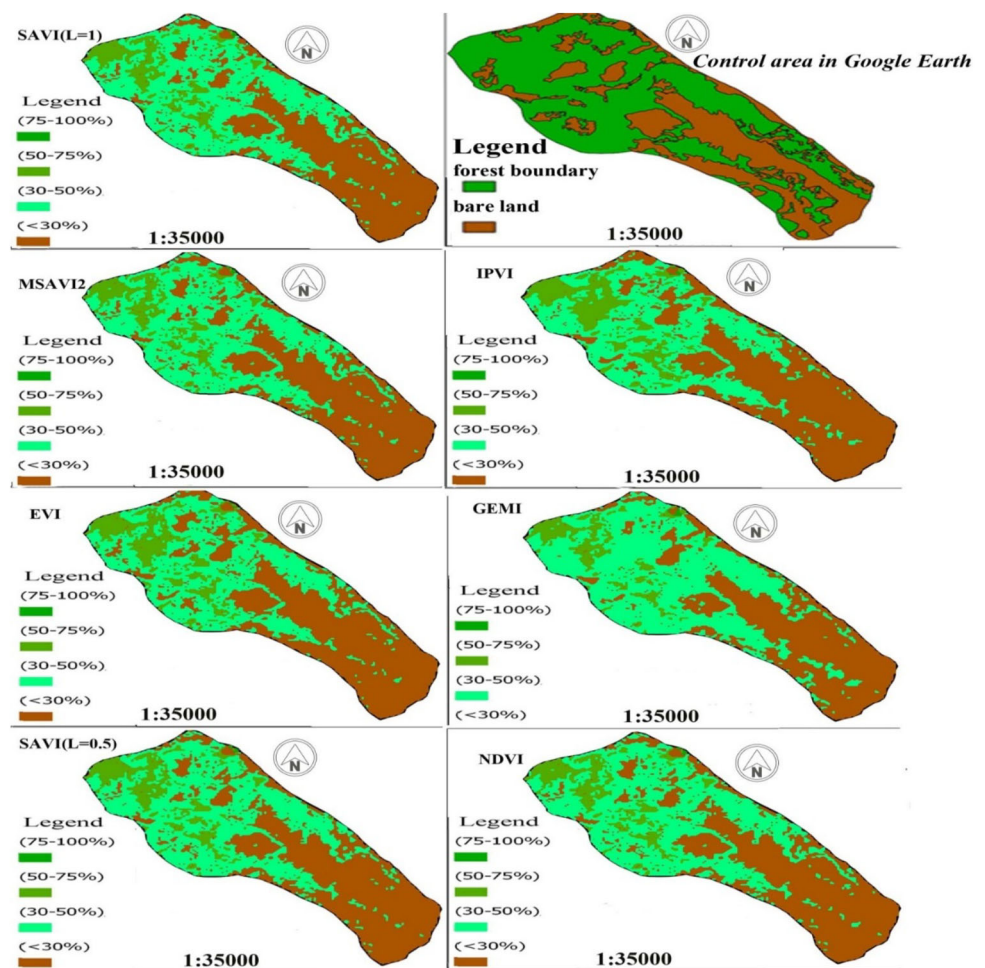


Table 6 Numerical value of indices in control area

Vegetation Indices	EVI	GEMI	IPVI	MSAVI2	NDVI	SAVI_05	SAVI_1
VI/Vi	0.86	0.99	0.87	0.92	0.85	0.90	0.93
Density of 50–75 %	105.975	74.149	120.04	89.887	119.94	96.525	92.486
Density of 30–50 %	389.359	499.297	380.486	440.415	370.462	422.617	445.151
Total	495.33	573.446	500.526	530.302	488.402	519.142	537.637

VI vegetation index, Vi visual interpretation

Fig. 4 Land-use changes for study period from GEMI

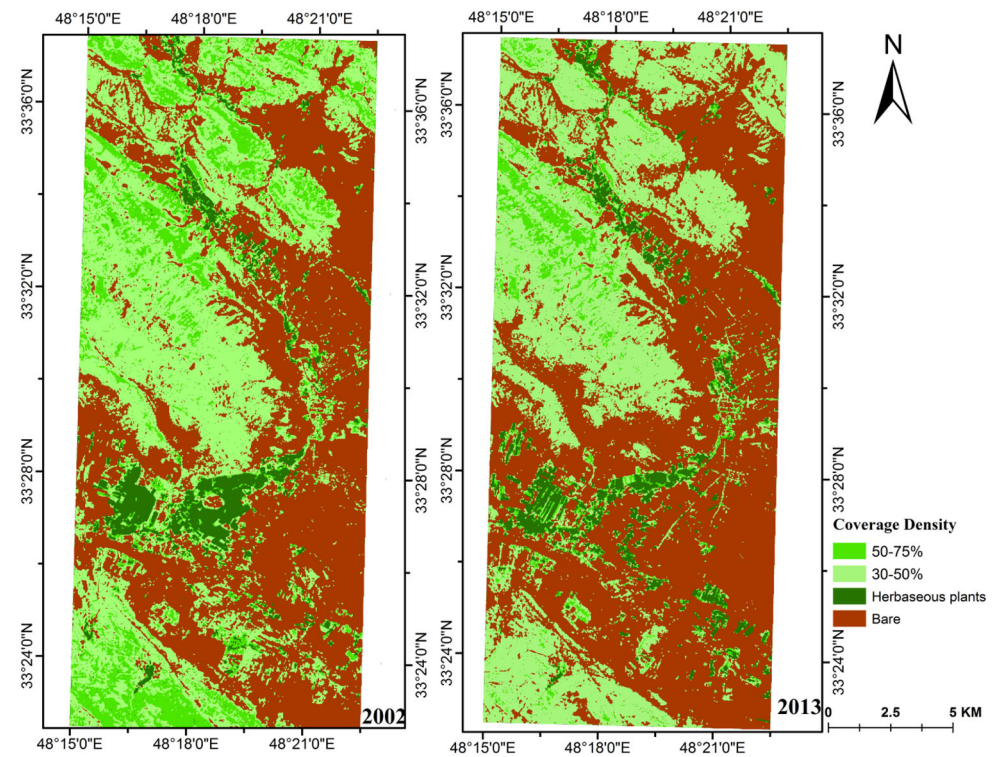


Table 7 Changes in coverage density of study area from GEMI

Cover	75–100 %	50–75 %	30–50 %	<30 %	Total forest area (ha)
2002	1934	3880	12,196	14,521	16,076
2013	1780	1580	11,776	17,095	13,356

The accuracy of indices depends on field studies and expertise for classification for image analysis. The results showed that the RMSE error rate in this study was very small and field studies showed high accuracy. The biomass density of trees as assessed for regions with similar geological conditions for the study region using the proposed formulas. As seen in thematic maps covering 11 years, the total area of the forest (with a density of 30–75 % of biomass) has decreased by 2720 ha² (16.91 %). It can be concluded that damaging agricultural methods near forests (Pourhashemi et al. 2004), inappropriate use of trees (Henareh Khalyani et al. 2014; Sadeghravesh et al. 2015), unsustainable exploitation of

water resources especially groundwater resources (Zehetabian et al. 2010; Mashayekhi et al. 2010; Shirmohammadi et al. 2013; Moosavi et al. 2013; Rahmati et al. 2016), misplaced structures (Zehetabian et al. 2014), and depletion of crops had increased desertification in the study region.

References

Adina T, Anne C, Birgit K, Michael F (2014) Estimation of the seasonal leaf area index in an alluvial forest using high-resolution satellite-based vegetation indices. *Remote Sens Environ* 141:52–63

- Ahmed OS, Franklin SE, Wulder MA, White JC (2015) Characterizing stand-level forest canopy cover and height using landsat time series, samples of airborne LiDAR, and the random forest algorithm. *ISPRS J Photogramm Remote Sens* 101:89–101
- Austin AT, Vivanco L (2006) Plant litter decomposition in a semi-arid ecosystem controlled by photo degradation. *Nature* 442(7102):555–558
- Bailey HP (1979) Semi-arid climates: their definition and distribution. *Agriculture in semi-arid environments*. Springer, Berlin, pp 73–97
- Beadle NCW (1959) Some aspects of ecological research in semi-arid Australia. *Biogeography and Ecology in Australia*. Springer, Dordrecht, pp 452–460
- Béland M, Baldocchi DD, Widlowski JL, Fournier RA, Verstraete MM (2014) On seeing the wood from the leaves and the role of voxel size in determining leaf area distribution of forests with terrestrial LiDAR. *Agric For Meteorol* 184:82–97
- Bradley BA, Mustard JF (2008) Comparisons of phenology trends by land cover class: a case study in the Great Basin, USA. *Glob Chang Biol* 14:334–346
- Brandt JS, Kuemmerle T, Li H, Ren G, Zhu J, Radeloff VC (2012) Using Landsat imagery to map forest change in southwest China in response to the national logging ban and ecotourism development. *Remote Sens Environ* 121:358–369
- Brantley ST, Zinnert JC, Young DR (2011) Application of hyperspectral vegetation indices to detect variations in high leaf area index temperate shrub thicket canopies. *Remote Sens Environ* 115(2):514–523
- Breshears D (2006) The grassland–forest continuum: trends in ecosystem properties for woody plant mosaics? *Front Ecol Environ* 4:96–104
- Chaban LN. 2004. Theory and algorithms pattern recognition. Moscow State University of Geodesy and Cartography, in (Russian)
- Chen JM, Black TA (1991) Measuring leaf area index of plant canopies with branch architecture. *Agric For Meteorol* 57:1–12
- Chen JM, Cihlar J (1996) Retrieving leaf area index of boreal conifer forests using Landsat TM images. *Remote Sens Environ* 55:153–162
- Cohen WB, Maiersperger TK, Gower ST, Turner DP (2003) An improved strategy for regression of biophysical variables and Landsat ETM + data. *Remote Sens Environ* 84:561–571
- Colombo R, Bellingeri D, Fasolini D, Marino CM (2003) Retrieval of leaf area index in different vegetation types using high resolution satellite data. *Remote Sens Environ* 86(1):120–131
- Coppin P, Jonckheere I, Nackaerts K, Muys B, Lambin E (2004) Digital change detection methods in ecosystem monitoring: a review. *Int J Remote Sens* 25(9):1565–1596
- Crippen RE (1990) Calculating the vegetation index faster. *Remote Sens Environ* 34:71–73
- Datt B (1999) A new reflectance index for remote sensing of chlorophyll content in higher plants: tests using Eucalyptus leaves. *J Plant Physiol* 154:30–36
- Diouf A, Lambin EF (2001) Monitoring land-cover changes in semi-arid regions: remote sensing data and field observations in the Ferlo, Senegal. *J Arid Environ* 48(2):129–148
- Ferreira MP, Alves DS, Shimabukuro YE (2015) Forest dynamics and land-use transitions in the Brazilian Atlantic Forest: the case of sugarcane expansion. *Reg Environ Chang* 15(2):365–377
- Franklin SE (2001) *Remote sensing for sustainable forest management*. CRC, Boca Raton
- Galvao LS, dos Santos JR, Roberts DA, Breunig FM, Toomey M, de Moura YM (2011) On intra-annual EVI variability in the dry season of tropical forest: a case study with MODIS and hyperspectral data. *Remote Sens Environ* 115(9):2350–2359
- Ghanbari S, Sefidi K (2012) Comparison of sustainable forest management (SFM) trends at global and country levels: case study in Iran. *J For Res* 23(2):311–317
- Griffiths P, Kuemmerle T, Baumann M, Radeloff VC, Abrudan IV, Lieskovsky J, Hostert P (2014) Forest disturbances, forest recovery, and changes in forest types across the Carpathian ecoregion from 1985 to 2010 based on Landsat image composites. *Remote Sens Environ* 151:72–88
- Heisler-White JL, Knapp AK, Kelly EF (2008) Increasing precipitation event size increases aboveground net primary productivity in a semi-arid grassland. *Oecologia* 158(1):129–140
- Henareh Khalyani A, Falkowski MJ, Mayer AL (2012) Classification of landsat images based on spectral and topographic variables for land-cover change detection in Zagros forests. *Int J Remote Sens* 33(21):6956–6974
- Henareh Khalyani J, Namiranian M, Heshmatol Vaezin SM, Feghhi J (2014) Development and evaluation of local communities incentive programs for improving the traditional forest management: a case study of Northern Zagros forests, Iran. *J For Res* 25(1):205–210
- Heumann BW, Seaquist JW, Eklundh L, Jonsson P (2007) AVHRR derived phenological change in the Sahel and Soudan, Africa, 1982–2005. *Remote Sens Environ* 108:385–392
- Homet-Gutiérrez P, Schupp EW, Gómez JM (2015) Naturalization of almond trees (*Prunus dulcis*) in semi-arid regions of the Western Mediterranean. *J Arid Environ* 113:108–113
- Hostert P, Röder A, Hill J (2003) Coupling spectral unmixing and trend analysis for monitoring of long-term vegetation dynamics in Mediterranean rangelands. *Remote Sens Environ* 87:183–197
- Huang CQ, Goward SN, Schleeweis K, Thomas N, Masek JG, Zhu ZL (2009) Dynamics of national forests assessed using the Landsat record: case studies in eastern United States. *Remote Sens Environ* 113:1430–1442
- Huete AR (1988) A Soil-Adjusted Vegetation Index (SAVI). *Remote Sens Environ* 25(3):295–309
- Jian Y, Peter J, Nathan A (2012) Landsat remote sensing approaches for monitoring long-term tree cover dynamics in semi-arid woodlands: comparison of vegetation indices and spectral mixture analysis. *Remote Sens Environ* 119:62–71
- Ko D, Bristow N, Greenwood D, Weisberg P (2009) Canopy cover estimation in semiarid woodlands: comparison of field-based and remote sensing methods. *For Sci* 55:132–141
- Lal R (2004) Carbon sequestration in dryland ecosystems. *Environ Manag* 33:528–544
- Lanorte A, Lasaponara R, Lovallo M, Telesca L (2014) Fisher-Shannon information plane analysis of SPOT/VEGETATION Normalized Difference Vegetation Index (NDVI) time series to characterize vegetation recovery after fire disturbance. *Int J Appl Earth Obs Geoinform* 26:441–446
- Le Maire G, Marsden C, Nouvellon Y, Grinand C, Hakamada R, Stape JL, Laclau JP (2011) MODIS NDVI time-series allow the monitoring of eucalyptus plantation biomass. *Remote Sens Environ* 115(10):2613–2625
- Letnic M, Laffan SW, Greenville AC, Russell BG, Mitchell B, Fleming PJ (2015) Artificial watering points are focal points for activity by an invasive herbivore but not native herbivores in conservation reserves in arid Australia. *Biodivers Conserv* 24(1):1–16
- Lillesand TM, Kiefer RW (1994) *Remote Sensing and Image Interpretation*. Wiley, New York, p 750
- Macleod RD, Congalton RG (1998) A quantitative comparison of change-detection algorithms for monitoring eelgrass from remotely sensed data. *Photogramm Eng Remote Sens* 64(3):207–216

- Mashayekhi Z, Panahi M, Karami M, Khalighi S, Malekian A (2010) Economic valuation of water storage function of forest ecosystems (case study: Zagros Forests, Iran). *J For Res* 21(3):293–300
- Moosavi V, Vafakhah M, Shirmohammadi B, Behnia N (2013) A wavelet-ANFIS hybrid model for groundwater level forecasting for different prediction periods. *Water Resour Manag* 27(5):1301–1321
- Mutanga O, Skidmore AK (2004) Narrow band vegetation indices overcome the saturation problem in biomass estimation. *Int J Remote Sens* 25(19):3999–4014
- Myneni RB, Keeling CD, Tucker CJ, Asrar G, Nemani RR (1997) Increased plant growth in the northern high latitudes from 1981 to 1991. *Nature* 386(6626):698–702
- Paruelo JM, Sala OE, Beltrán AB (2000) Long-term dynamics of water and carbon in semi-arid ecosystems: a gradient analysis in the Patagonian steppe. *Plant Ecol* 150(1–2):133–143
- Peters AJ, Walter-Shea EA, Ji L, Vina A, Hayes M, Svoboda MD (2002) Drought monitoring with NDVI-based standardized vegetation index. *Photogramm Eng Remote Sens* 68(1):71–75
- Pinty B, Verstraete MM (1992) GEMI: a non-linear index to monitor global vegetation from satellites. *Vegetation* 101(1):15–20
- Potitsep S, Nagai S, Nasahara KN, Muraoka H, Suzuki R (2013) Two separate periods of the LAI–VIs relationships using in situ measurements in a deciduous broadleaf forest. *Agric For Meteorol* 169:148–155
- Pourhashemi M, Marvi Mohajer MR, Zobeiri M, Amiri GZ, Panahi P (2004) Identification of forest vegetation units in support of government management objectives in Zagros forests, Iran. *Scand J For Res* 19(S4):72–77
- Qi J, Chehbouni A, Huete AR, Kerr YH, Sorooshian S (1994) A modified soil adjusted vegetation index. *Remote Sens Environ* 48(2):119–126
- Rahmati O, Pourghasemi HR, Melesse AM (2016) Application of GIS-based data driven random forest and maximum entropy models for groundwater potential mapping: a case study at Mehran Region, Iran. *CATENA* 137:360–372
- Richards JA (1993) An introduction to remote sensing digital image analysis, 2nd edn. Springer, New York, p 225
- Riha KM, Michalski G, Gallo EL, Lohse KA, Brooks P, Meixner T (2014) High atmospheric nitrate inputs and nitrogen turnover in semi-arid urban catchments. *Ecosystems* 17(8):1309–1325
- Roni R (2013) Surface temperature and NDVI generation and relation between them: application of remote sensing. *Asian J Eng Technol Innov* 1(1):08–13
- Rotenberg E, Yakir D (2010) Contribution of semi-arid forests to the climate system. *Science* 327(5964):451–454
- Rouse J 1974 Monitoring the Vernal Advancement and Retrogradation (Green Wave Effect) of Natural Vegetation NASA/GSFC Type III Final Report, Greenbelt, MD, 371p
- Sadeghravesh MH, Khosravi H, Ghasemian S (2015) Application of fuzzy analytical hierarchy process for assessment of combating-desertification alternatives in central Iran. *Nat Hazards* 75(1):653–667
- Saranya KRL, Reddy CS, Rao PP, Jha CS (2014) Decadal time-scale monitoring of forest fires in Similipal Biosphere Reserve, India using remote sensing and GIS. *Environ Monit Assess* 186(5):3283–3296
- Schmidt M, Lucas R, Bunting P, Verbesselt J, Armston J (2015) Multi-resolution time series imagery for forest disturbance and regrowth monitoring in Queensland, Australia. *Remote Sens Environ* 158:156–168
- Sexton JO, Song XP, Feng M, Noojipady P, Anand A, Huang C, Townshend JR (2013) Global, 30-m resolution continuous fields of tree cover: landsat-based rescaling of MODIS vegetation continuous fields with lidar-based estimates of error. *Int J Digit Earth* 6(5):427–448
- Shirmohammadi B, Vafakhah M, Moosavi V, Moghaddamnia A (2013) Application of several data-driven techniques for predicting groundwater level. *Water Resour Manag* 27(2):419–432
- Singh A (1989) Review article digital change detection techniques using remotely-sensed data. *Int J Remote Sens* 10(6):989–1003
- Slayback DA, Pinzon JE, Los SO, Tucker CJ (2003) Northern hemisphere photosynthetic trends 1982–99. *Glob Chang Biol* 9:1–15
- Starr G, Staudhammer CL, Loescher HW, Mitchell R, Whelan A, Hiers JK, O'Brien JJ (2015) Time series analysis of forest carbon dynamics: recovery of *Pinus palustris* physiology following a prescribed fire. *New For* 46(1):63–90
- Sulla-Menashe D, Kennedy RE, Yang Z, Braaten J, Krankina ON, Friedl MA (2014) Detecting forest disturbance in the Pacific Northwest from MODIS time series using temporal segmentation. *Remote Sens Environ* 151:114–123
- Tang H, Broly M, Zhao F, Strahler AH, Schaaf CL, Ganguly S, Dubayah R (2014) Deriving and validating Leaf Area Index (LAI) at multiple spatial scales through lidar remote sensing: a case study in Sierra National Forest, CA. *Remote Sens Environ* 143:131–141
- Thenkabail PS, Lyon JG, Huete A (2016) Hyperspectral remote sensing of vegetation. CRC Press
- Torahi AA, Rai SC (2011) Land cover classification and forest change analysis, using satellite imagery—a case study in Dehdez area of Zagros mountain in Iran. *J Geogr Inf Syst* 3(01):1
- Tucker CJ (1979) Red and photographic infrared linear combinations for monitoring vegetation. *Remote Sens Environ* 8:127–150
- Walker BH (2012) Management of semi-arid ecosystems. Elsevier, Amsterdam
- Walker JJ, De Beurs KM, Wynne RH, Gao F (2012) Evaluation of Landsat and MODIS data fusion products for analysis of dryland forest phenology. *Remote Sens Environ* 117:381–393
- Zehtabian G, Khosravi H, Ghodsi M (2010) High demand in a land of water scarcity: Iran. *Water and Sustainability in Arid Regions*. Springer, Dordrecht, pp 75–86
- Zehtabian G, Khosravi H, Masoodi R (2014) Desertification assessment models (Criteria and indicators). University of Tehran Press, Iran (In Farsi), Tehran
- Zhu Z, Woodcock CE, Olofsson P (2012) Continuous monitoring of forest disturbance using all available Landsat imagery. *Remote Sens Environ* 122:75–91